Supplementary Information

Tumor-derived small extracellular vesicles inhibit the efficacy of CAR T cells against solid tumors

Wenqun Zhong, Zebin Xiao, Zhiyuan Qin, Jingbo Yang, Yi Wen, Ziyan Yu, Yumei Li, Neil C. Sheppard, Serge Y. Fuchs, Xiaowei Xu, Meenhard Herlyn, Carl H. June, Ellen Puré, and Wei Guo
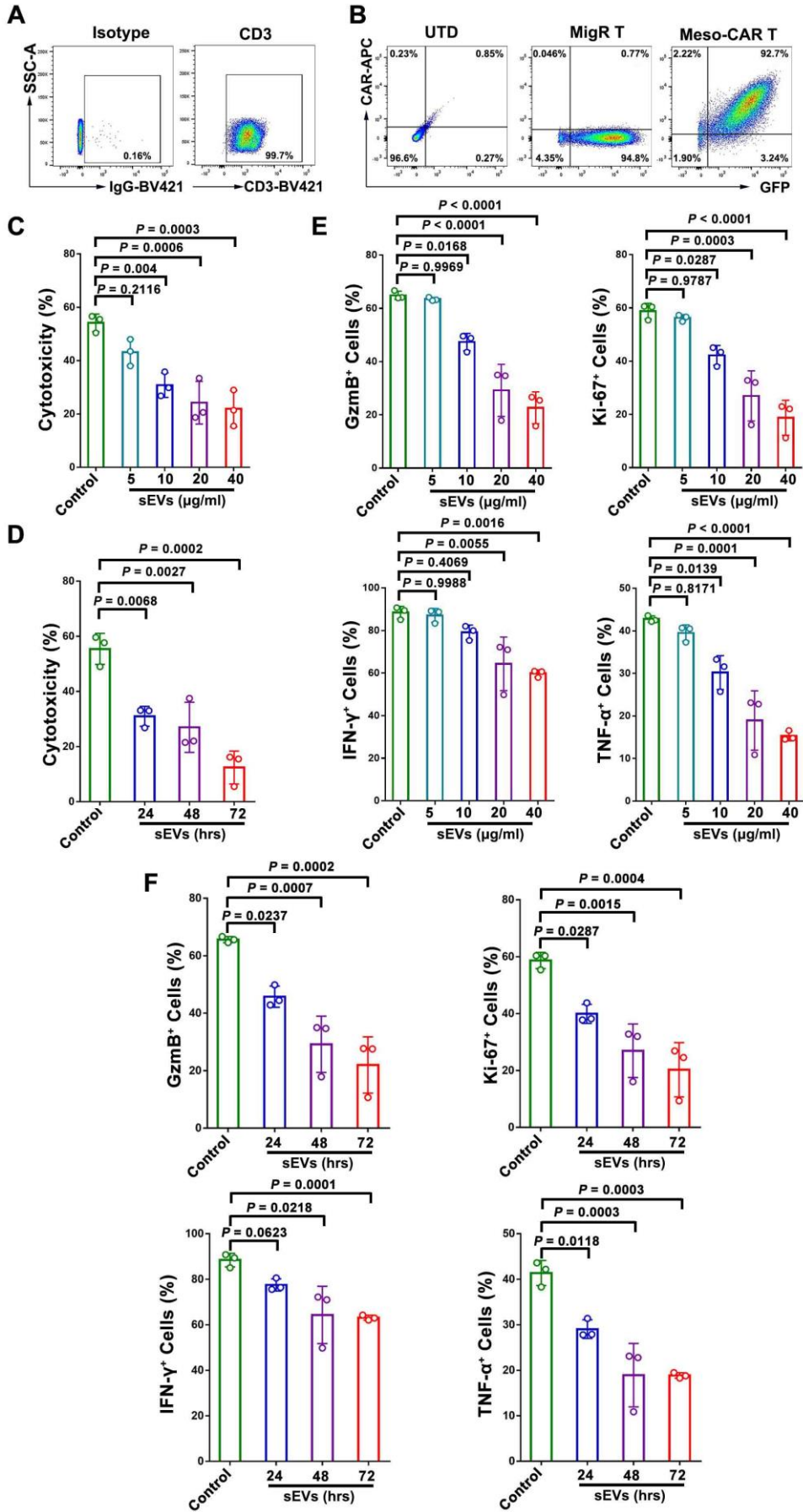
Figure S1. sEVs released from 4662 cells inhibit Meso-CAR T cells in a dose and time-dependent manner. A, Purity of isolated mouse T cells used in the study, as analyzed by CD3$^+$ cells using flow cytometry. **B,** The percentage of cells expressing Meso-CAR-GFP or MigR-GFP. **C.** Meso-CAR T cells were first treated with 5, 10, 20 and 40 µg/ml 4662 cell-derived sEVs, and then co-cultured with 4662 cells for 48 hrs. Apoptosis of tumor cells was detected by flow cytometry analysis of cleaved caspase-3. **D.** Meso-CAR T cells were first treated with 20 µg/ml 4662 cell-derived sEVs for 24, 48 and 72 hrs, and then co-cultured with 4662 cells for 48 hrs. Apoptosis of tumor cells detected by flow cytometry analysis of cleaved caspase-3 is shown. **E,** Quantification of cells with GzmB, Ki-67, IFN-γ and TNF-α expression in Meso-CAR T cells after treatments with indicated amounts of 4662 cell-derived sEVs. **F,** Quantification of cells with GzmB, Ki-67, IFN-γ and TNF-α expression in Meso-CAR T cells after indicated hours of treatments with 4662 cell-derived sEVs. Statistical analysis is performed using Welch ANOVA with Sidak's T3 multiple comparison tests **(C-F).**
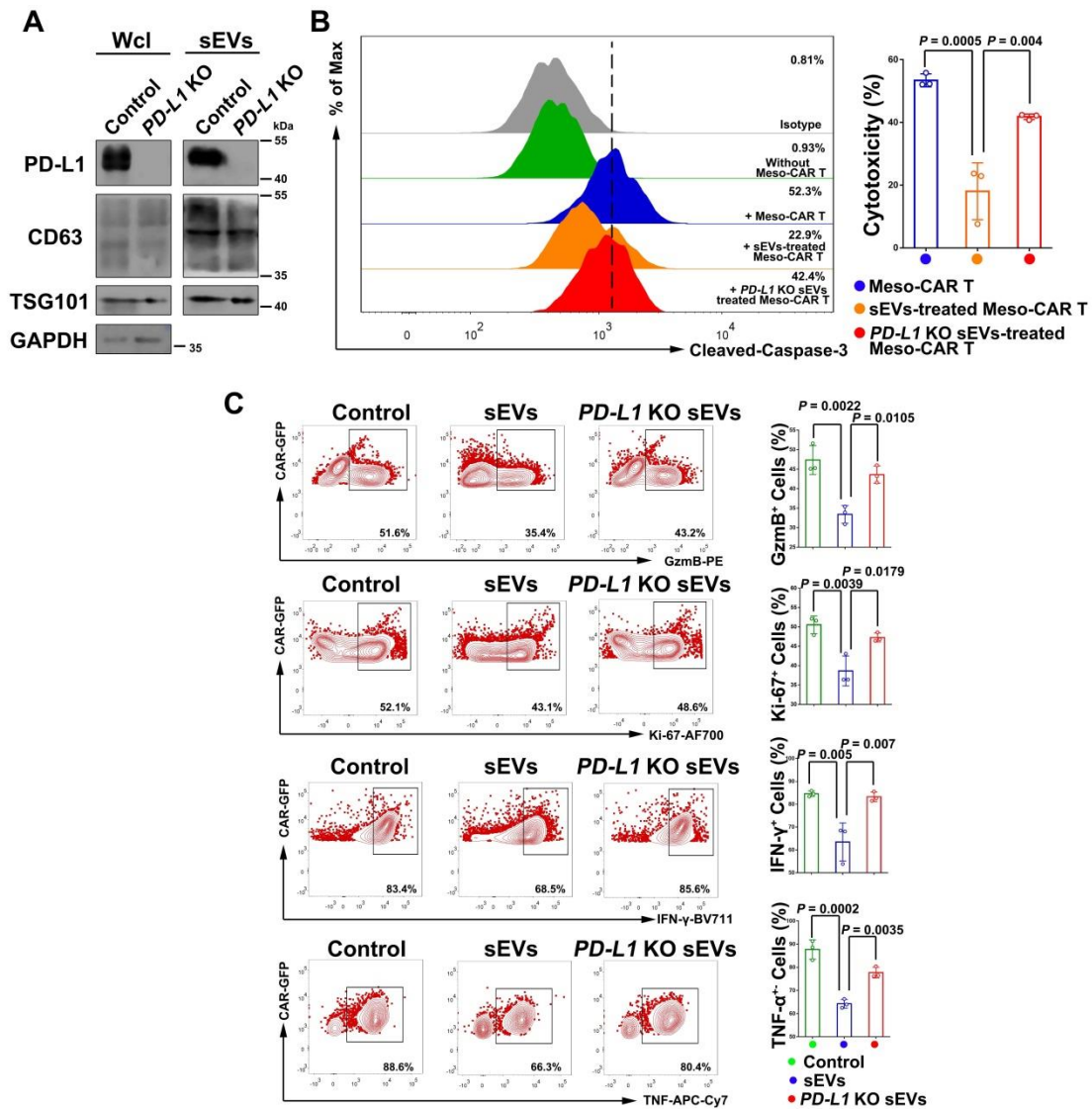
Figure S2. sEVs released from 4662 cells inhibit Meso-CAR T cells. A, Immunoblot analysis of PD-L1 and exosome markers (CD63 and TSG101) in the whole cell lysate ("Wcl") and purified sEVs from control and *PD-L1* knockout ("*PD-L1* KO") 4662 cells. The same amounts of proteins were loaded in each lane. **B,** Meso-CAR T cells were first treated with PBS, sEVs, sEVs with or without *PD-L1* KO, and then co-cultured with 4662 cells for 48 hrs. Apoptosis of tumor cells detected by flow cytometry analysis of cleaved caspase-3 is shown (left panel), and the relative cytotoxicity is calculated (right panel). **C,** Representative flow cytometric images of Meso-CAR T cells examined for the expression of GzmB, Ki-67, IFN-γ and TNF-α after indicated treatments. Quantification of cells with positive GzmB, Ki-67, IFN-γ and TNF-α expression in Meso-CAR T cells after indicated treatments is shown at the right. Data represent mean ± s.d. (n=3). Statistical analysis is performed using one-way ANOVA analysis with Dunnett's multiple comparison tests **(B, C).**
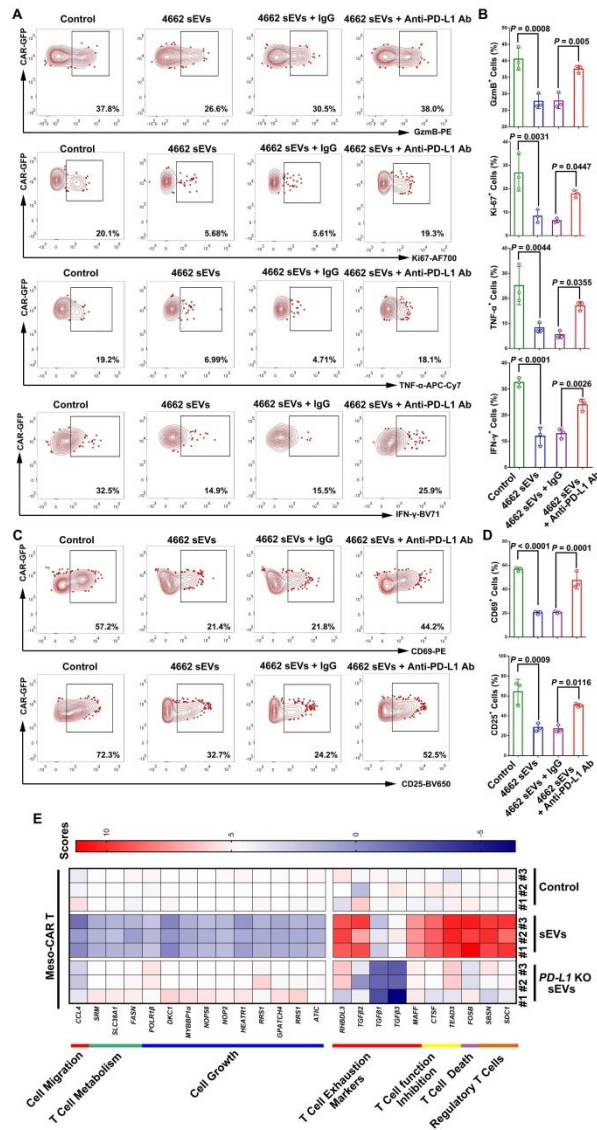
Figure S3. Tumor cell-derived sEVs had a significantly inhibitory effect on the activation of CAR T cells. A, Meso-CAR T cells were treated with a smaller amount of CD3/CD28 beads to achieve lower levels of activation (see Materials and Methods for details). Representative flow cytometry images of Meso-CAR T cells examined for the expression of GzmB, Ki-67, interferon gamma (IFN-γ) and tumor necrosis factor-α (TNF-α) after indicated treatments with sEVs derived from 4662 cells. **B,** Quantification of cells with GzmB, Ki-67, TNF-α and IFN-γ expression in Meso-CAR T cells after indicated treatments is shown. **C,** Representative flow cytometry images of Meso-CAR T cells examined for the expression of CD69 and CD25 after indicated treatments. Quantification of cells with CD69 and CD25 expression in Meso-CAR T cells after indicated treatments is shown to the right. **D,** Quantification of Meso-CAR T cells with CD69 and CD25 expression by flow cytometry analysis. **E,** Heatmap showing the expression levels of the representative genes in Meso-CAR T cells with or with indicated sEV treatment. Data represent mean ± s.d. (n=3). Statistical analysis is performed using Welch ANOVA with Sidak's T3 multiple comparison tests **(B, D)**.
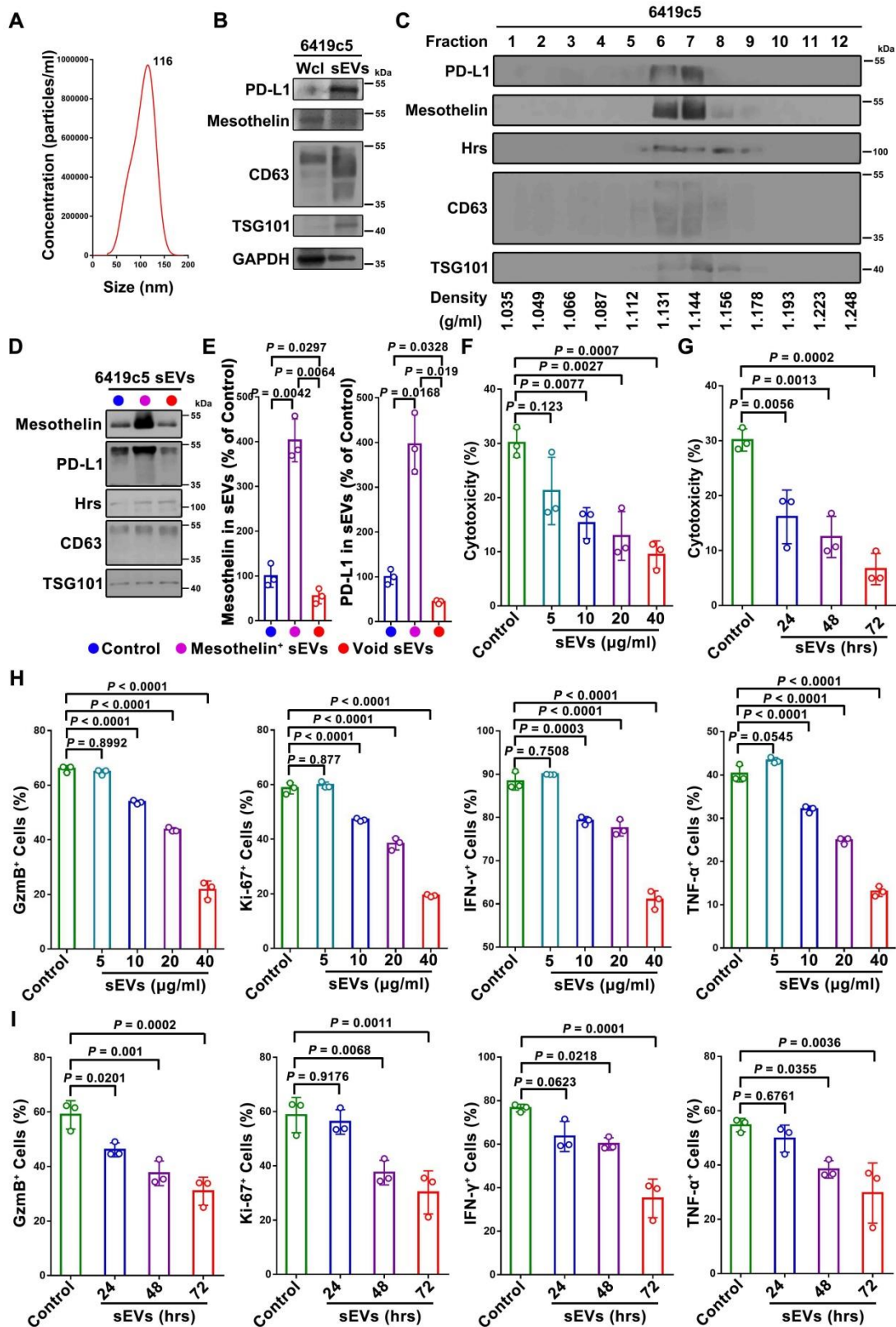
Figure S4. sEVs released from 6419c5 cells inhibit Meso-CAR T cells. A, Nanoparticle tracking analysis of sEVs purified from 6419c5 cells. The X-axis represents the diameters of the particles and the Y-axis represents the concentration (particles/ml) of the sEVs. **B,** Western blot analysis of PD-L1, mesothelin and exosome marker proteins (CD63 and TSG101) in the

whole cell lysate ("Wcl"), and purified sEVs from 6419c5 cells. All lanes were loaded with equal amounts of proteins. **C,** PD-L1 and mesothelin co-fractionated with exosome marker proteins (Hrs, CD63 and TSG101) on density gradients from 6419c5 cell-derived sEVs. **D,** Enrichment of mesothelin$^+$ sEVs from 6419c5 cell-derived sEVs by magnetic beads. See Materials and Methods for details. Characterization of mesothelin$^+$ sEVs and remaining ("Void sEVs") sEVs by western blotting. The expression levels of mesothelin and exosome marker proteins (Hrs, CD63 and TSG101) in indicated sEVs are shown. An equal amount of sEV proteins from the different fractions was loaded on the gel. **E,** Quantification of sEV mesothelin (left) and PD-L1 (right) levels in 6419c5 cell-derived sEVs in different fractions. **F,** Meso-CAR T cells were treated with PBS, 5, 10, 20 and 40 µg/ml of 6419c5 cell-derived sEVs, and then co-cultured with 6419c5 cells for 48 hrs. Apoptosis of 6419c5 cells was assayed by flow cytometry using cleaved caspase-3. Relative cytotoxicity is shown. **G,** Meso-CAR T cells treated with PBS or 20 µg/ml 6419c5 cell-derived sEVs for 24, 48 and 72 hrs, and then co-cultured with 6419c5 cells for 48 hrs. Apoptosis of 6419c5 cells was assayed by flow cytometry using cleaved caspase-3. Relative cytotoxicity is shown. **H,** Quantification of cells with GzmB, Ki-67, IFN-γ and TNF-α expression in Meso-CAR T cells treated with PBS, or 5, 10, 20 and 40 µg/ml sEVs derived from 6419c5 cells. **I,** Quantification of cells with GzmB, Ki-67, IFN-γ and TNF-α expression in Meso-CAR T cells treated with PBS or 20 µg/ml sEVs derived from 6419c5 cells for 24, 48 and 72 hrs. Statistical analysis is performed using one-way ANOVA analysis with Dunnett's multiple comparison tests **(E)**, Welch ANOVA with Sidak's T3 multiple comparison tests **(F-I)**.
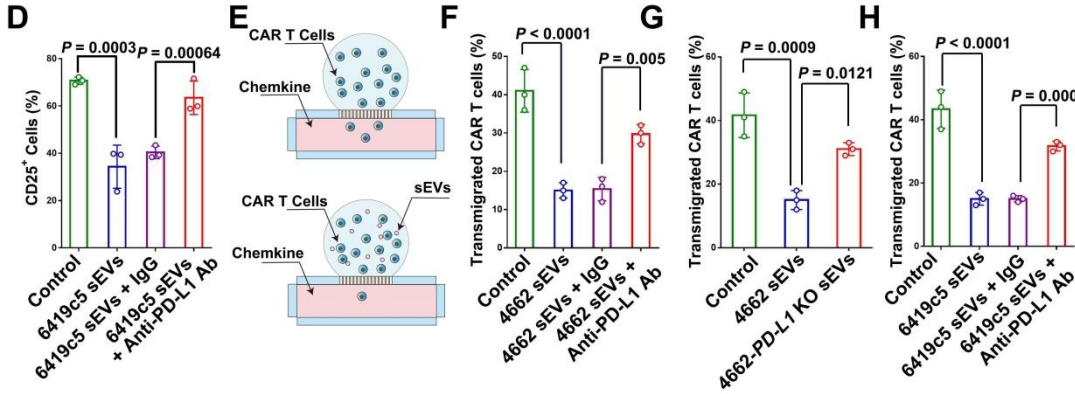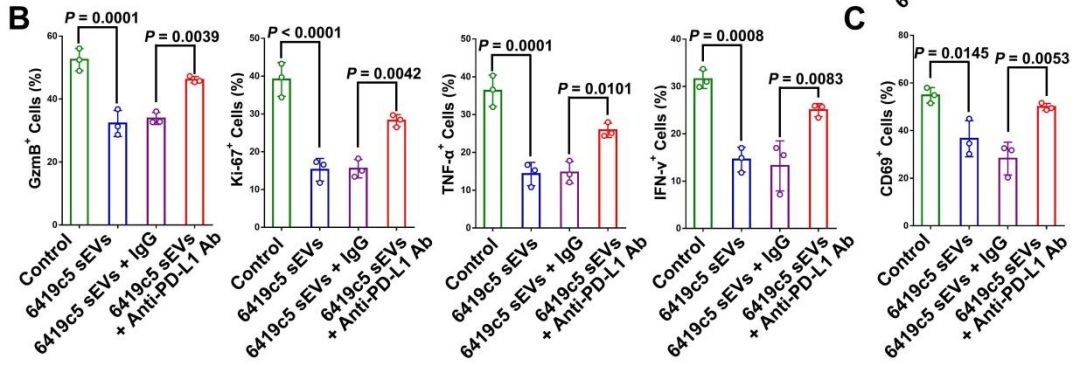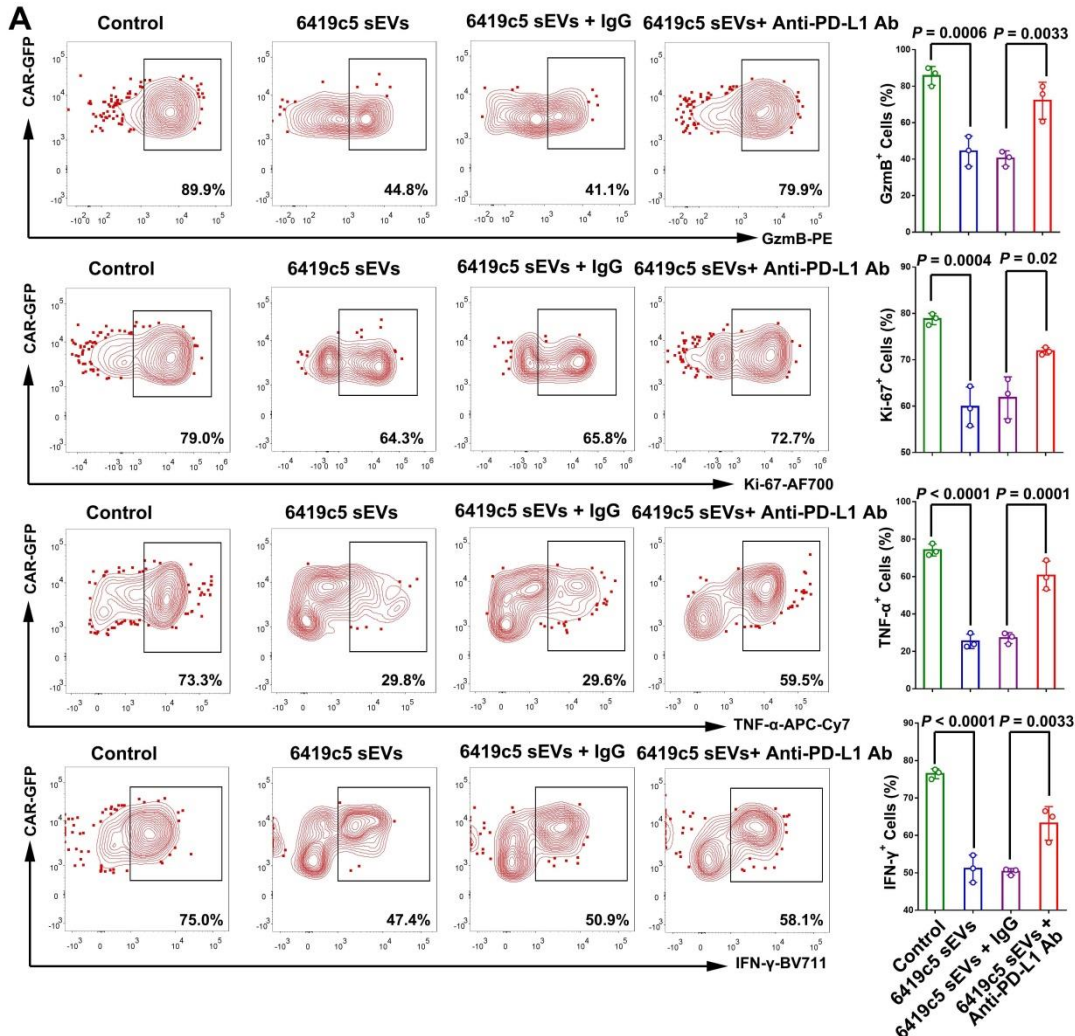
Figure S5. PD-L1 mediates the inhibition of Meso-CAR T cells by sEVs. A, Representative flow cytometric images of Meso-CAR T cells examined for the expression of GzmB, Ki-67, TNF-α and IFN-γ after indicated treatments. Quantification of cells with positive GzmB, Ki-67, TNF-α and IFN-γ expression in Meso-CART cells after indicated treatments is shown at the right. **B,** Meso-CAR T cells were treated with a smaller amount of CD3/CD28 beads to achieve lower levels of activation (see Materials and Methods for details). Representative flow cytometry images of Meso-CAR T cells examined for the expression of GzmB, Ki-67, tumor necrosis factor-α (TNF-α) and interferon gamma (IFN-γ) after indicated treatments with sEVs derived from 6419c5 cells. Quantification of cells with GzmB, Ki-67, TNF-α and IFN-γ expression in Meso-CAR T cells after indicated treatments is shown. **C,** Quantification of cells with CD69 expression in Meso-CAR T cells after indicated treatments is shown. **D,** Quantification of cells with CD25 expression in Meso-CAR T cells after indicated treatments is shown. **E,** Schema for the chemotaxis assay for Meso-CAR T cells migration with (above) or without (below) tumor cell-derived sEV treatment (See the details in Materials and Methods). **F** and **G,** Percentages of transmigrated Meso-CAR T cells treated with or without indicated sEVs derived from 4662 cells in chemotaxis assay. **H,** Percentages of transmigrated Meso-CAR T cells treated with or without indicated sEVs derived from 6419c5 cells in chemotaxis assay. Data represent mean ± s.d. (n=3). Statistical analysis is performed using Welch ANOVA with Sidak's T3 multiple comparison tests **(A-D, F, H)**, or one-way ANOVA analysis with Dunnett's multiple comparison tests **(G)**.
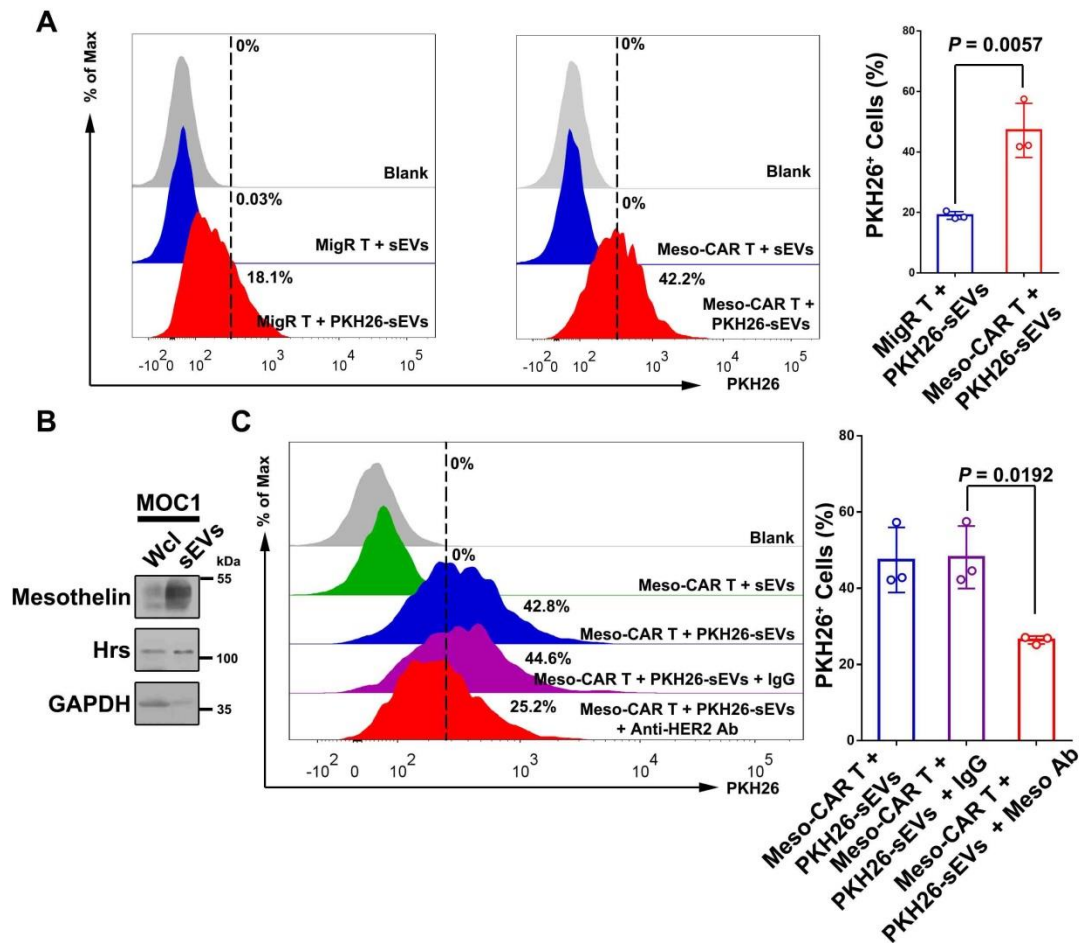
Figure S6. Mesothelin mediates the adhesion of MOC1 cell-derived sEVs to Meso-CAR T cells. A, Representative images of flow cytometry of MigR T cells and Meso-CAR T cells after incubation with PKH26-labeled MOC1 cell-derived sEVs. Quantification of the proportion of sEV-bound MigR T cells and Meso-CAR T cells is shown to the right. **B,** Western blot showing sEVs derived from MOC1 cells contain mesothelin. The same amounts of proteins were loaded in each lane. **C,** Representative images of flow cytometry of MigR T cells and Meso-CAR T cells after incubation with PKH26-labeled MOC1 cell-derived sEVs, which were treated with or without IgG or anti-mesothelin antibody. Quantification of the percentages of sEV-bound HER2-CAR T cells is shown to the right. Data represent mean ± s.d. (n=3). Statistical analysis is performed using two-sided unpaired *t*-test **(A)** or one-way ANOVA analysis with Dunnett's multiple comparison tests **(C)**.
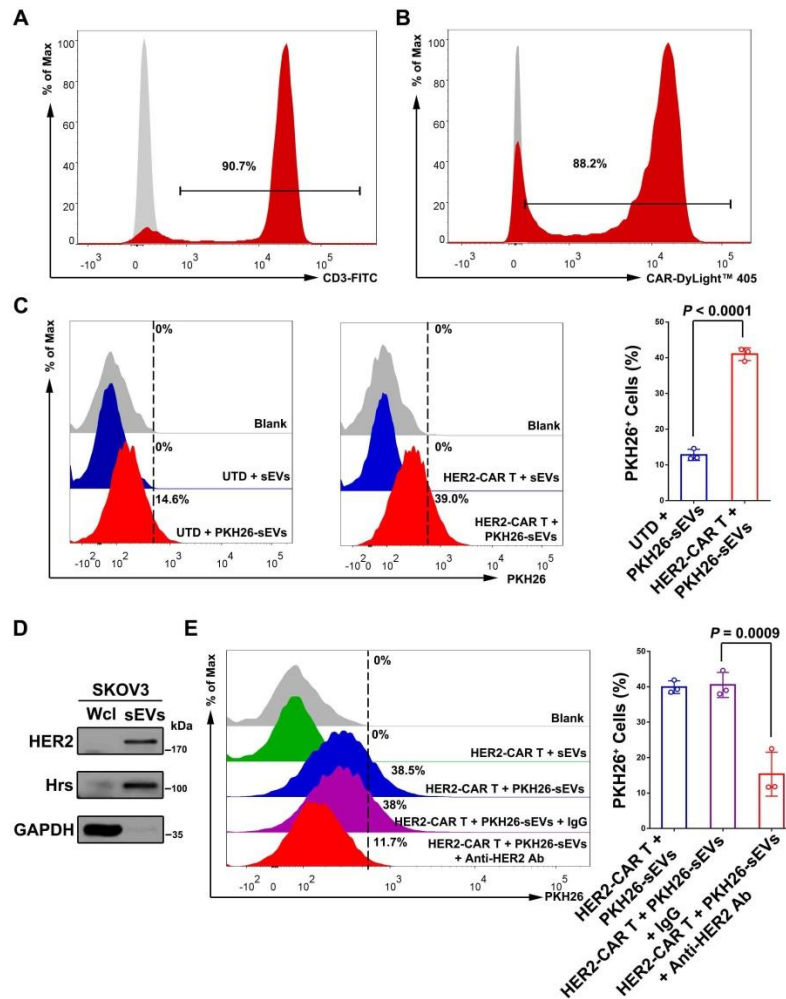
Figure S7. HER2 mediates the adhesion of SKOV3 cell-derived sEVs to HER2-CAR T cells. A, The purity of isolated human T cells used in the study. **B,** Transfection efficiency of human HER2-CAR T cells. **C,** Representative images of flow cytometry of untransduced ("UTD") and HER2-CAR T cells after incubation with PKH26-labeled SKOV3 cell-derived sEVs. Quantification of the proportion of sEV-bound UTD control and HER2-CAR T cells is shown to the right. **D,** Western blot showing sEVs derived from SKOV3 cells had high level of HER2 in the sEVs. The same amounts of proteins were loaded in each lane. **E,** Representative images of flow cytometry of control cells UTD and HER2-CART cells after incubation with PKH26-labeled SKOV3 cell-derived sEVs, which were treated with or without IgG or anti-HER2 antibody. Quantification of the percentages of sEV-bound UTD control and HER2-CAR T cells is shown to the right. Data represent mean ± s.d. (n=3). Statistical analysis is performed using two-sided unpaired *t*-test **(C)** or one-way ANOVA analysis with Dunnett's multiple comparison tests **(E)**.
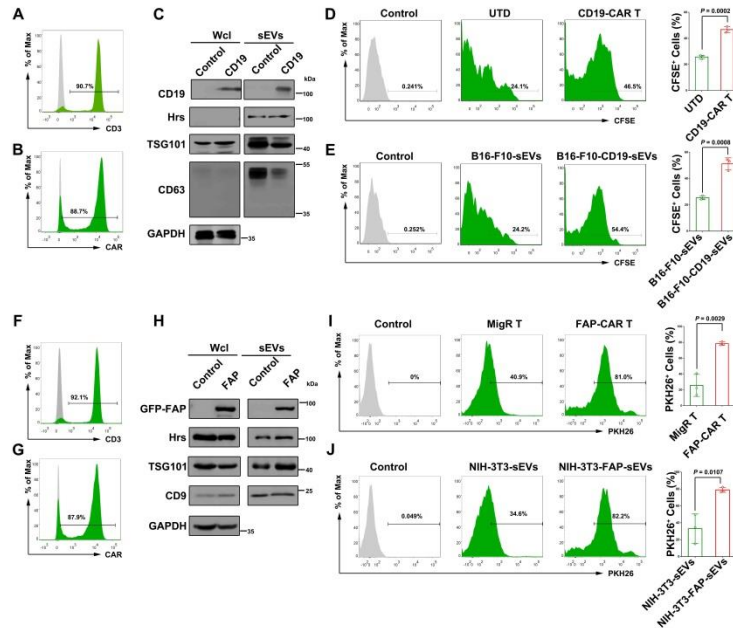
Figure S8. CD19 and FAP regulated the adhesion of sEVs to the CD19-CAR or FAP-CAR T cells, respectively. A, The purity of isolated mouse T cells used in the study. **B,** Transfection efficiency of mouse CD19-CAR. **C,** Western blot showing sEVs derived from B16-F10-CD19 cells had higher level of CD19 compared to the control cells. **D,** Representative images of flow cytometry of untransduced T cells ("UTD") and CD19-CAR T cells after incubation with CFSE-labeled B16-F10-CD19 cell-derived sEVs. Quantification of the percentages of sEV-bound UTD and CD19-CAR T cells is shown at the right. **E,** Representative images of flow cytometry of CD19-CAR T cells after incubation with CFSE-labeled B16-F10 or B16-F10-CD19 cell-derived sEVs. Quantification of the percentages of sEV-bound UTD and CD19-CAR T cells is shown at the right. **F,** The purity of isolated mouse T cells used in the study. **G,** Transfection efficiency of mouse CD19-CAR. **H,** Western blot showing sEVs derived from NIH-3T3-FAP cells had a higher level of FAP compared to control cells. **I,** Representative images of flow cytometry of MigR T cells (MigR T) and FAP-CAR T cells after incubation with PKH26-labeled NIH-3T3-FAP cell-derived sEVs. Quantification of the percentages of sEV-bound MigR T cells and FAP-CAR T cells is shown at the right. **J,** Representative images of flow cytometry of FAP-CAR T cells after incubation with PKH26-labeled NIH-3T3 or NIH-3T3-FAP cell-derived sEVs. Quantification of the percentages of sEV-bound control cells and FAP-CAR T cells is shown to the right. Data represent mean ± s.d. (n=3). Statistical analysis is performed using two-sided unpaired t-test **(D, E, I, J).**
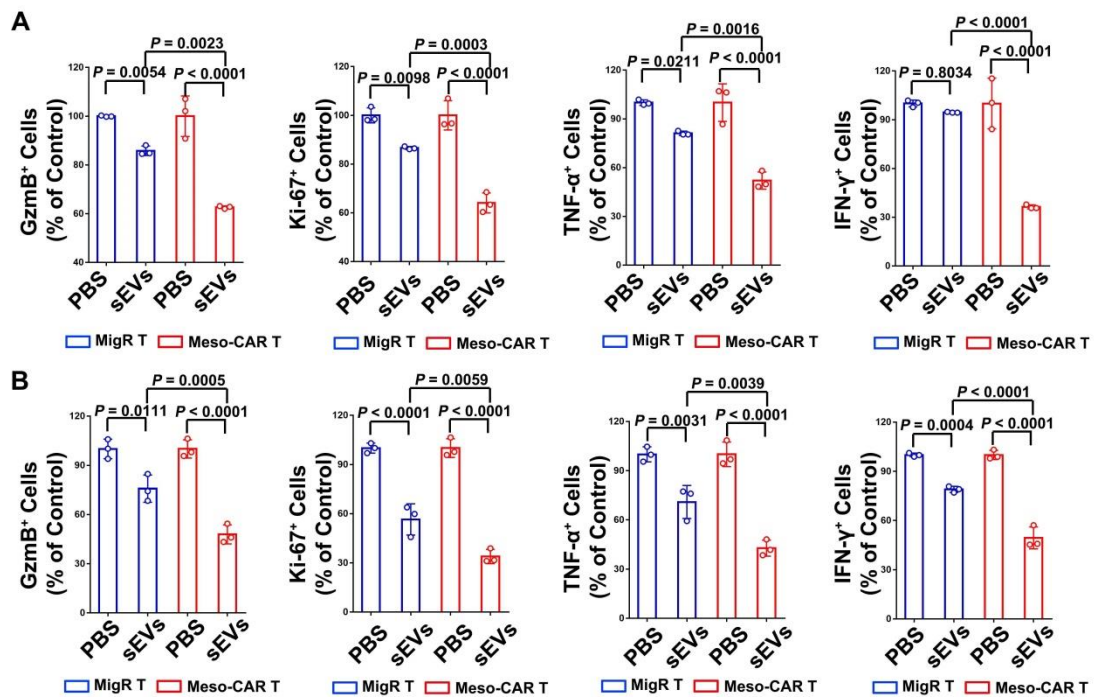
Figure S9. sEVs from 6419c5 cells and MOC1 cells had a stronger inhibitory effect on Meso-CAR T cells than MigR T cells. A, Quantification of MigR T cells and Meso-CAR T cells with GzmB, Ki-67, TNF-α and IFN-γ expression after indicated 6419c5-derived sEV treatments. **B,** Quantification of MigR T cells and Meso-CAR T cells with GzmB, Ki-67, TNF-α and IFN-γ expression after indicated treatments with MOC1-derived sEVs. Data represent mean ± s.d. (n=3). Statistical analysis was performed using Welch ANOVA with Sidak's T3 multiple comparison tests **(A, B).**

Figure S10. Mesothelin contributes to the tumor killing of CAR T cells by 6419c5 cell and MOC1 cell-derived sEVs. A, Meso-CAR T cells treated with PBS, sEVs, sEVs with or without IgG isotype or anti-mesothelin antibody blocking were co-cultured with 6419c5 cells for 48 hrs. Apoptosis of tumor cells detected by flow cytometry analysis of cleaved caspase-3 is shown to the left. The relative cytotoxicity is calculated and shown to the right. **B,** Meso-CAR T cells treated with PBS, sEVs, sEVs with or without IgG isotype or anti-mesothelin antibody blocking were co-cultured with MOC1 cells for 48 hrs. Apoptosis of tumor cells detected by flow cytometry analysis of cleaved caspase-3 is shown to the left. The relative cytotoxicity is calculated and shown to the right. Data represent mean ± s.d. (n=3). Statistical analysis was performed using Welch ANOVA with Sidak's T3 multiple comparison tests **(A, B).**
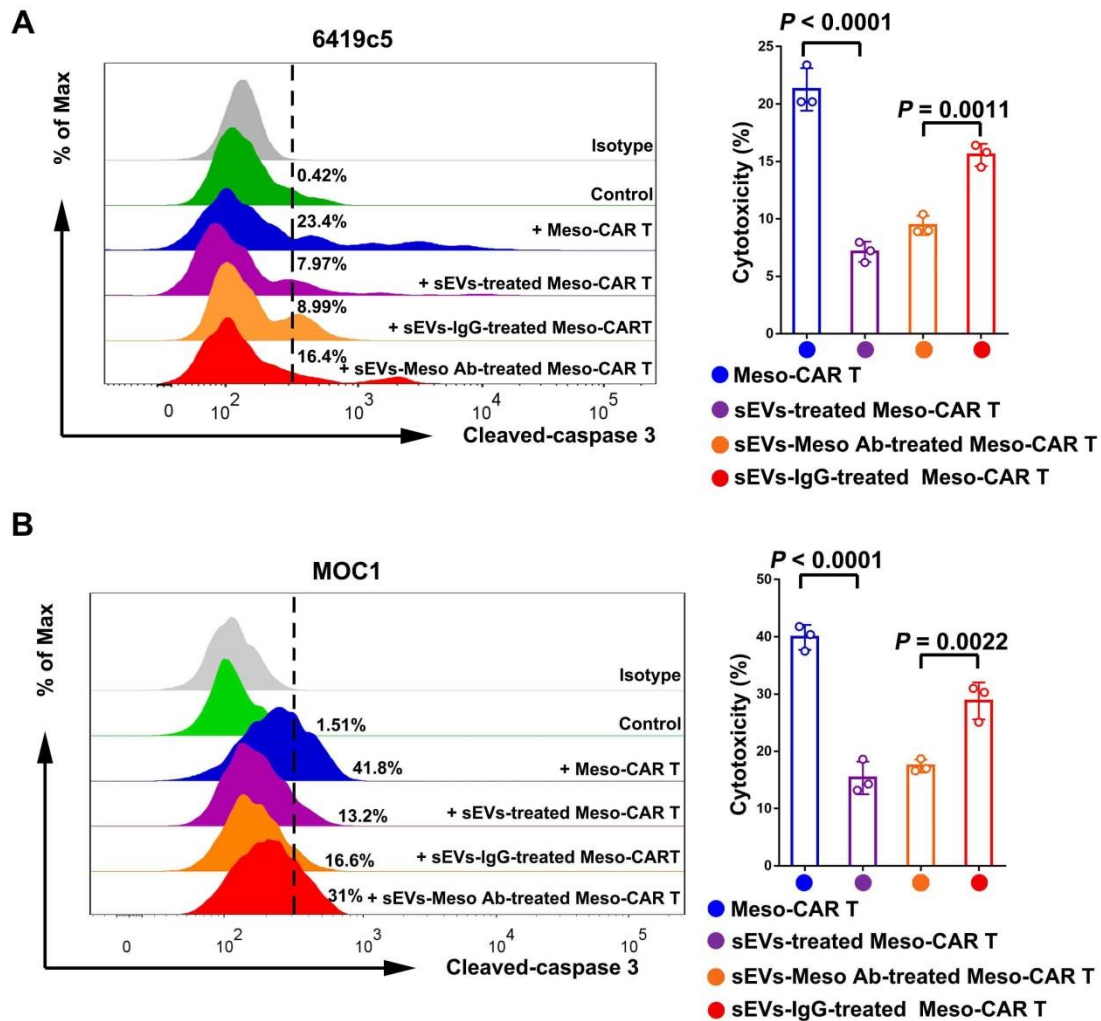
Figure S11. Mesothelin contributes to the preferential inhibition of CAR T cells by MOC1 cell-derived sEVs. A, Quantification of Meso-CAR T cells with GzmB, Ki-67, TNF-α and IFN-γ expression after indicated treatments. sEVs were purified from 6419c5 cells. **B,** Quantification of Meso-CAR T cells with GzmB, Ki-67, TNF-α and IFN-γ expression after indicated treatments. sEVs were purified from MOC1 cells. Data represent mean ± s.d. (n=3). Statistical analysis was performed using Welch ANOVA with Sidak's T3 multiple comparison tests **(A, B).**
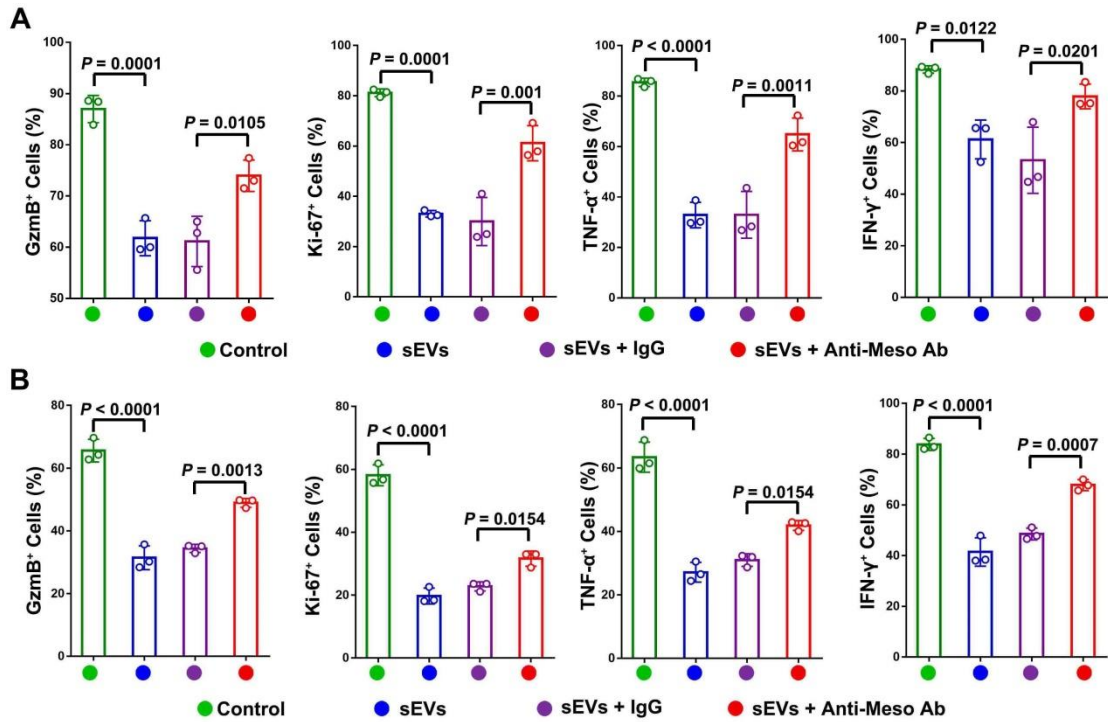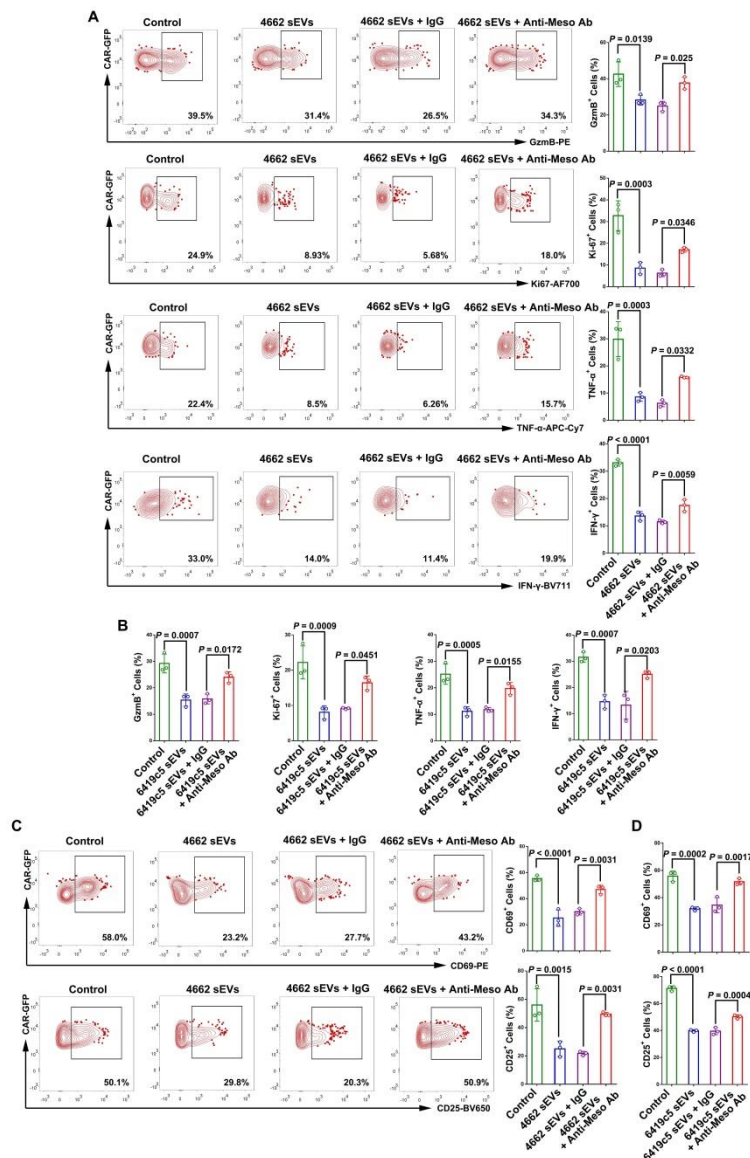
Figure S12. sEV mesothelin contributes to the inhibitory effect on the activation of CAR T cells. A, Meso-CAR T cells were treated with a smaller amount of CD3/CD28 beads to achieve lower levels of activation. Representative flow cytometry images of Meso-CAR T cells examined for the expression of GzmB, Ki-67, tumor necrosis factor-α (TNF-α) and interferon gamma (IFN-γ) after different treatments with sEVs derived from 4662 cells. Quantification of Meso-CAR T cells with GzmB, Ki-67, TNF-α and IFN-γ expression is shown to the right. **B,** Quantification of Meso-CAR T cells with GzmB, Ki-67, TNF-α and IFN-γ expression after treatments with 6419c4 cell derived sEVs. **C,** Representative flow cytometry images of Meso-CAR T cells examined for their expression of CD69 and CD25 after indicated treatment with sEVs derived from 4662 cells. Quantification of cells with CD69 and CD25 expression in Meso-CAR T cells is shown to the right. **D,** Quantification of Meso-CAR T cell CD69 and CD25 expression after treatments with sEVs derived from 6419c5 cells. Data represent mean ± s.d. (n=3). Statistical analysis is performed using Welch ANOVA with Sidak's T3 multiple comparison tests (**A-D**).
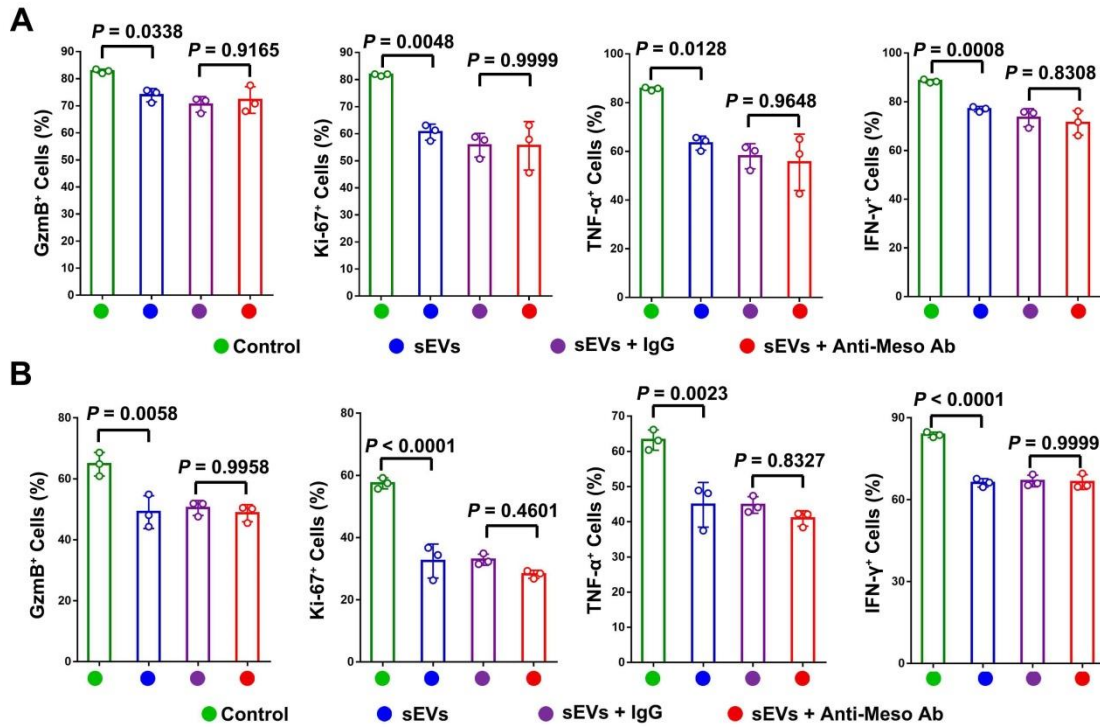
Figure S13. Mesothelin has no significant inhibitory effect of tumor cell-derived sEVs on MigR T cells. A, Quantification of MigR T cells with GzmB, Ki-67, TNF-α and IFN-γ expression after indicated treatments. sEVs were purified from 6419c5 cells. **B,** Quantification of MigR T cells with GzmB, Ki-67, TNF-α and IFN-γ expression after indicated treatments. sEVs were purified from MOC1 cells. Data represent mean ± s.d. (n=3). Statistical analysis is performed using Welch ANOVA with Sidak's T3 multiple comparison tests **(A, B)**.
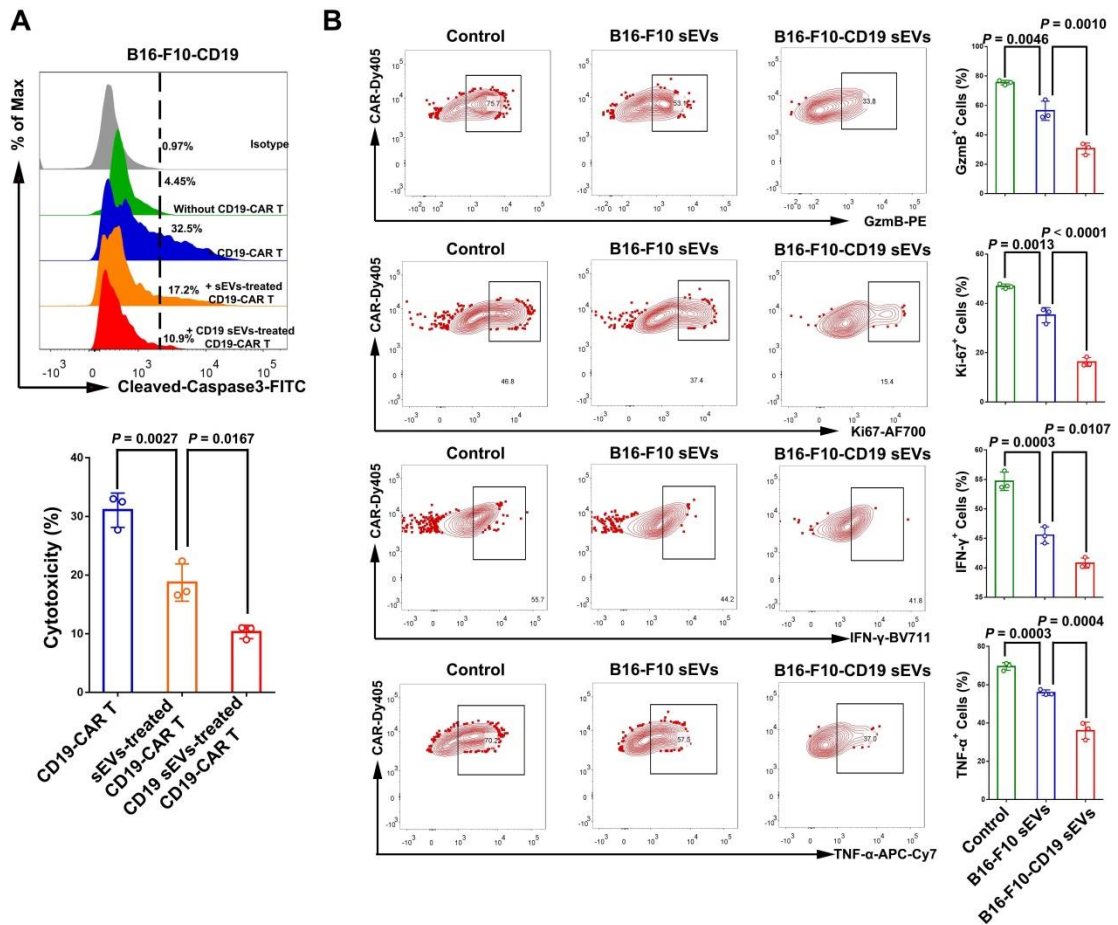
Figure S14. CD19 enhances the inhibitory effect of sEVs on CD19-CAR T cells. A, CD19-CAR T cells treated with PBS, sEVs derived from B16-F10 or B16-F10-CD19 cells were co-cultured with B16-F10-CD19 cells for 48 hrs. Apoptosis of tumor cells was detected by flow cytometry analysis of cleaved caspase-3 (upper panel), and the relative cytotoxicity was calculated (lower panel). **B,** Representative flow cytometry images of CD19-CAR T cells examined for the expression of GzmB, Ki-67, IFN-γ and TNF-α after indicated treatments. Quantification of cells with GzmB, Ki-67, IFN-γ and TNF-α expression in CD19-CAR T cells after indicated treatments is shown at the right. Data represent mean ± s.d. (n=3). Statistical analysis was performed using one-way ANOVA analysis with Dunnett's multiple comparison tests **(A, B)**.

A

Rab27a

GAPDH

kDa

— 25

— 35

Control

RAB27A KO

B

sEVs Per Cell

P = 0.0008

Control   RAB27A KO

C

% of Max

Control   98.7%

RAB27A KO   99.9%

Mesothelin

Mesothelin⁺ Cells (%)

P = 0.0554

Control   RAB27A KO

D

Tumor Volume (mm³)

WT tumor
RAB27A KO tumor

P = 0.7652

Days

E

Tumor Weight (g)

P < 0.0001
P < 0.0001
P = 0.44
P < 0.0001

MigR T   Meso-CAR T   MigR T   Meso-CAR T

WT Tumor   RAB27A KO Tumor

F

Tumor Volume (mm³)

WT Tumor   PBS
RAB27A KO   PBS
Tumor   12.5 µg sEVs
25 µg sEVs
50 µg sEVs

P < 0.0001
P = 0.188
P < 0.0001
P = 0.0002
P = 0.07130
P = 0.9862

Days

G

Tumor Weight (g)

P = 0.6338
P = 0.9461
P < 0.0001
P < 0.0001
P < 0.0001
P = 0.8999

WT Tumor + PBS   PBS   12.5   25   50

sEVs (µg/ml)

RAB27A KO Tumor

H

P = 0.0204
P = 0.0064
P = 0.3442
P = 0.0204

MigR T   WT Tumor
Meso-CAR T
MigR T   RAB27A KO Tumor
Meso-CAR T

Survival Rate (%)

Days

I

Cell: 78.4%

SSC-A

FSC-A

Single Cell: 98.4%

FSC-H

FSC-A

Live Cell: 71.0%

FSC-A

Live/Dead

GFP

Meso-CAR T Cell: 1.98%
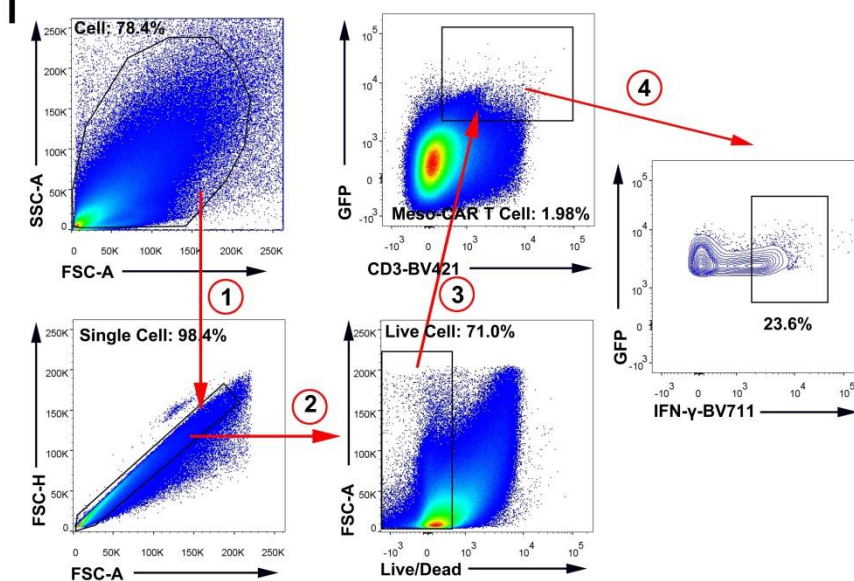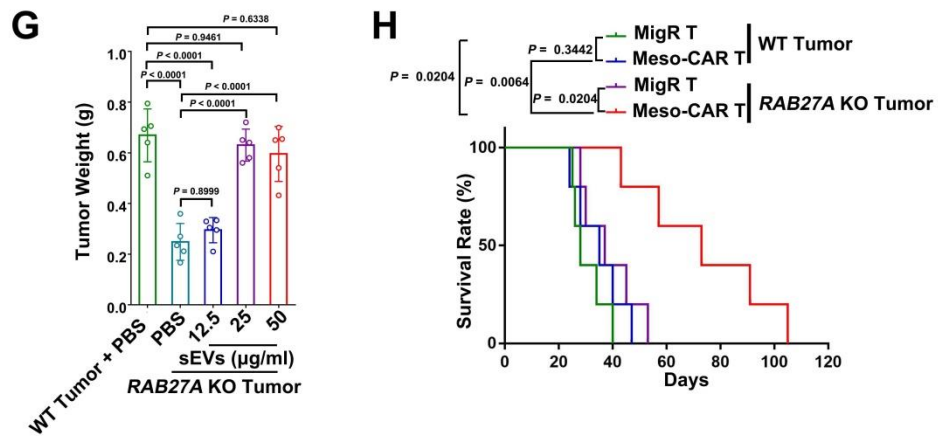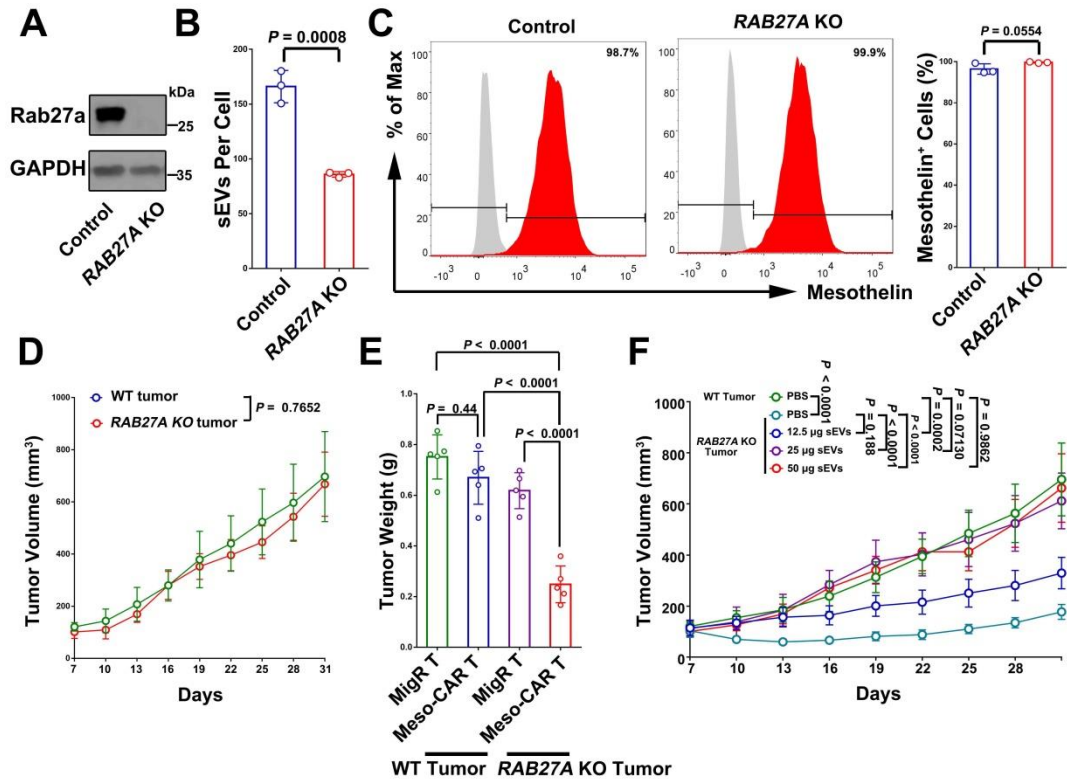
CD3-BV421

GFP

IFN-γ-BV711

23.6%

Figure S15. Knockout of *RAB27A* (*RAB27A* KO) improved the therapeutic effect of Meso-CAR T cells without affecting surface expression of mesothelin. A, Immunoblot analysis of Rab27a in the whole cell lysate from control and *RAB27A* knockout ("*RAB27A* KO") 4662 cells. **B,** Quantification of sEVs release from 4662 cells with or without *RAB27A* KO by nanoparticle tracking analysis. **C,** Representative flow cytometry images of 4662 cells with or without *RAB27A* KO. Quantification of cells with positive mesothelin expression in 4662 cells after indicated treatment is shown to the right (n=3). **D,** Tumor growth of 4662 cells with or without *RAB27A* KO in mice (n=5). **E,** Tumor weights with indicated treatment (n=5). **F,** Growth curves of tumors in mice with indicated treatments. **G,** Tumor weights with indicated treatments. **H,** Survival rates of mice with indicated treatments (n=5). **I,** Representative contour plots showing the general gating strategy used in the analysis of IFN-γ$^+$ Meso-CAR T cells. Data represent mean ± s.d. Statistical analysis is performed using two-sided unpaired *t*-test **(B, C, D)**, or Welch ANOVA with Dunnett's T3 multiple comparison tests **(E-G)** or log-rank test **(H)**.
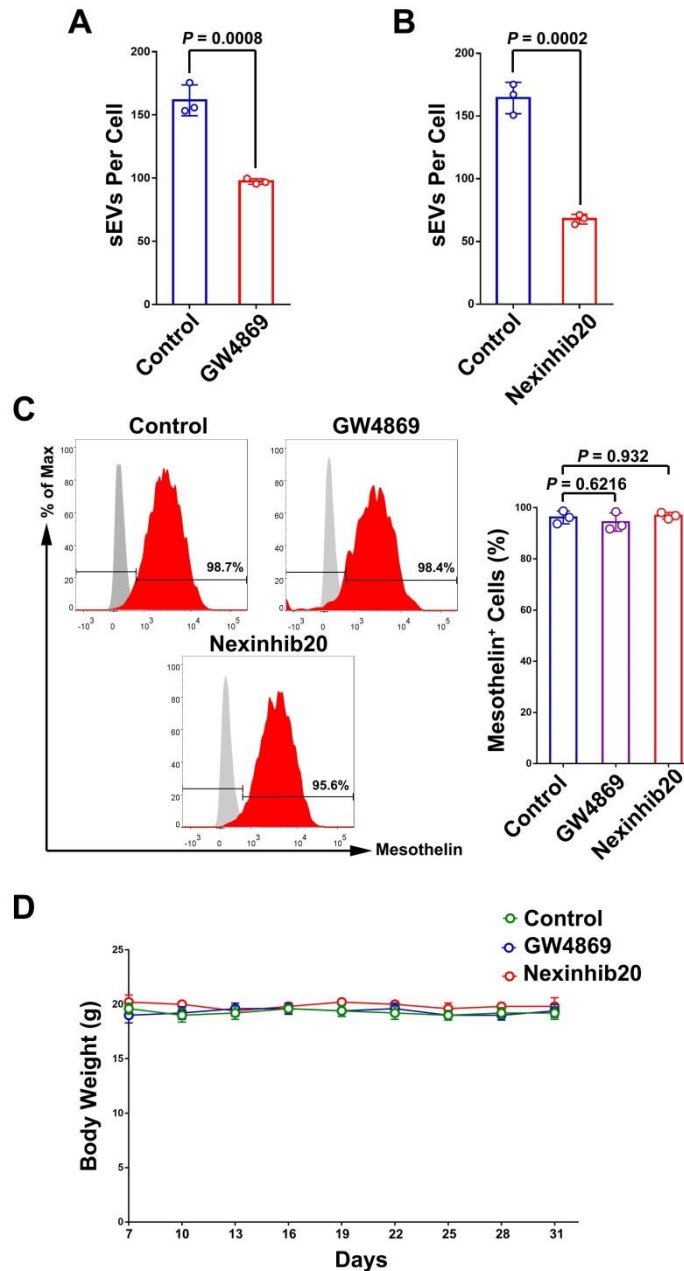
Figure S16. GW4869 and Nexinhib20 inhibited sEV secretion from 4662 cells without affecting the surface expression of mesothelin. A and **B,** Quantification of sEV release from 4662 cells with or without GW4869 treatment (**A**) or Nexinhib20 treatment (**B**) using nanoparticle tracking analysis. **C,** Representative flow cytometry images of 4662 cells with or without GW4869 or Nexinhib20 treatment. Quantification of cells with positive mesothelin expression in 4662 cells after indicated treatments is shown at the right. **D,** Body weight of mice with or without GW4869 or Nexinhib20 treatment (n=5). Data represent mean ± s.d. (n=3 or indicated). Statistical analysis is performed using two-sided unpaired *t*-test **(A, B),** or one-way ANOVA analysis with Dunnett's multiple comparison tests **(C, D)**.
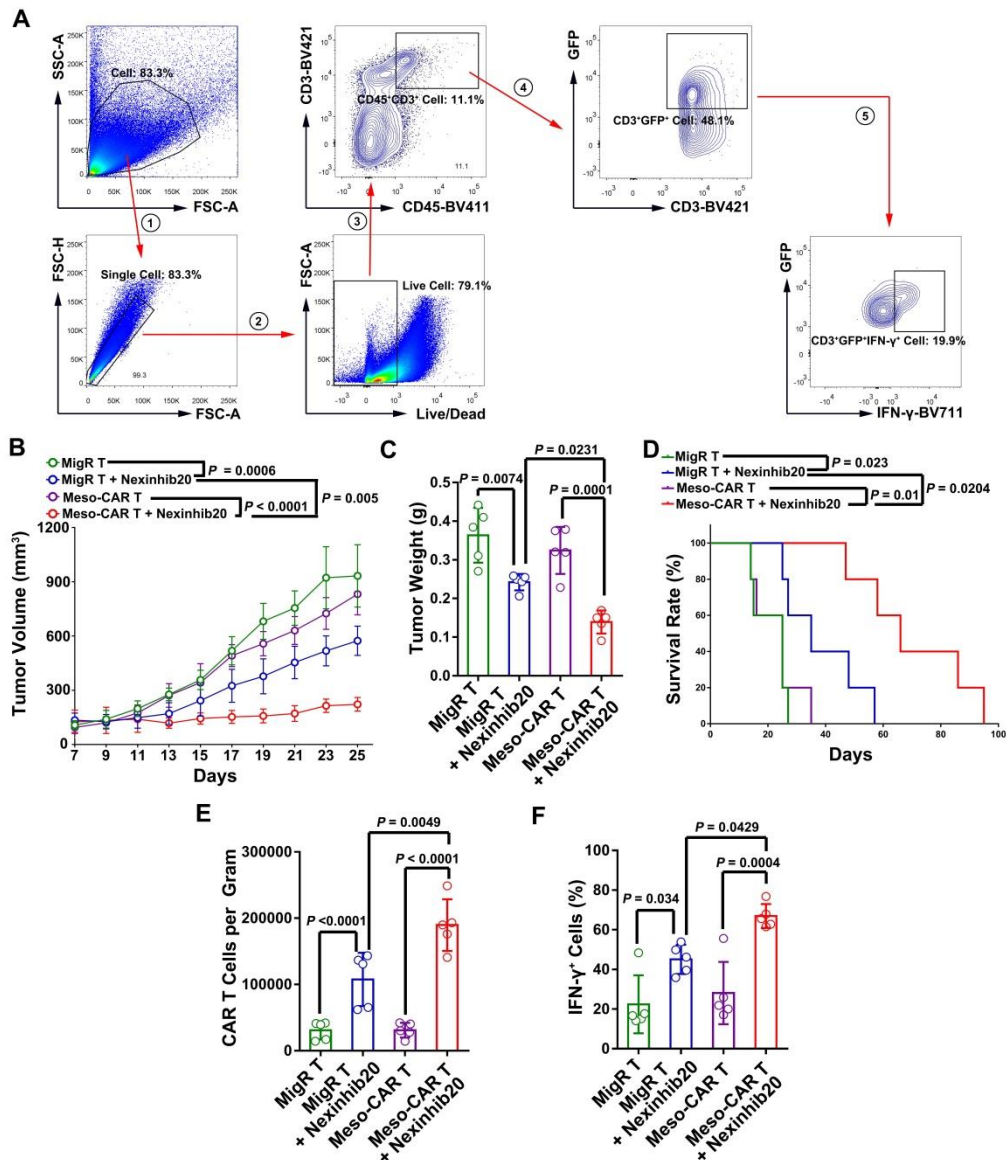
Figure S17. Nexinhib20 boosted CAR T therapy in a PDAC mouse model. A, Representative contour plots showing the general gating strategy used in the analysis of total Meso-CAR T cells, and IFN-γ$^+$ Meso-CAR T cells in C57BL/6 mice with 4662 xenografts. **B,** Tumor growth in mice with indicated treatments. **C,** Tumor weights in mice with indicated treatment. **D,** Survival rates of mice with indicated treatments. **E,** The number of Meso-CART cells in tumors for each group of mice quantified from flow cytometry analysis. **F,** The percentages of IFN-γ$^+$ Meso-CART cells quantified by flow cytometry. Data represent mean ± s.d. (n=5). Statistical analysis is performed using Welch ANOVA with Dunnett's T3 multiple comparison tests **(B, C, E, F)** or log-rank test **(D)**.
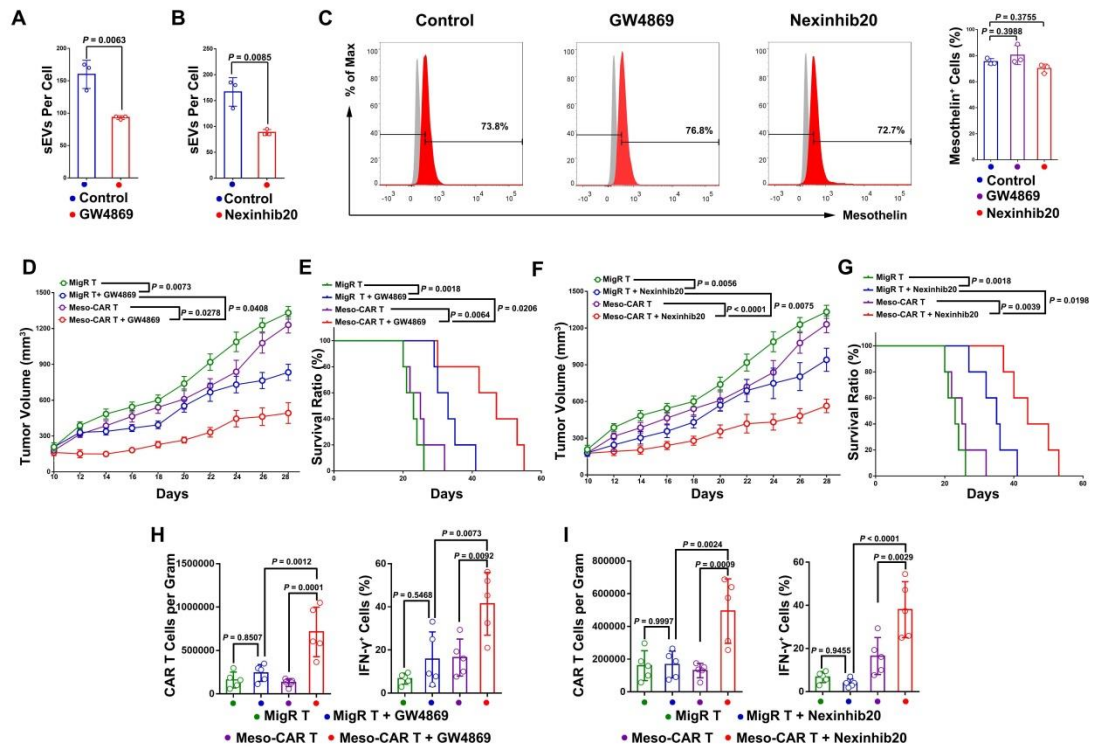
Figure S18. GW4869 and Nexinhib20 boosted CAR T therapy in a murine oral squamous cell carcinoma model. A and **B,** Quantification of sEV release from MOC1 cells with or without GW4869 treatment (**A**) or Nexinhib20 treatment (**B**) using nanoparticle tracking analysis. **C,** Representative flow cytometry images of mesothelin positive MOC1 cells with or without GW4869 or Nexinhib20 treatment. Quantification of cells with positive mesothelin expression in MOC1 cells after indicated treatments is shown at the right. **D,** Tumor growth in C57BL/6 mice with indicated GW4869 treatments. **E,** Survival rates of mice with indicated GW4869 treatments. **F,** Tumor growth in mice with indicated Nexinhib20 treatments. **G,** Survival rates of mice with indicated Nexinhib20 treatments. **H,** Related to GW4869 treatment, quantification of flow cytometry analysis of the number of Meso-CART cells in tumors for each group of mice (left panel), and the percentages of IFN-γ⁺ Meso-CART cells (right panel). **I,** Related to Nexinhib20 treatment, quantification of flow cytometry analysis of the number of Meso-CART cells in tumors for each group of mice (left panel), and the percentages of IFN-γ⁺ Meso-CART cells (right panel). Data represent mean ± s.d. (**D-I,** n=5). Statistical analysis is performed using two-sided unpaired *t*-test **(A, B),** or one-way ANOVA analysis with Dunnett's multiple comparison tests **(C)**, Welch ANOVA with Dunnett's T3 multiple comparison tests **(D, F, H, I)**, log-rank test **(E, G)**.
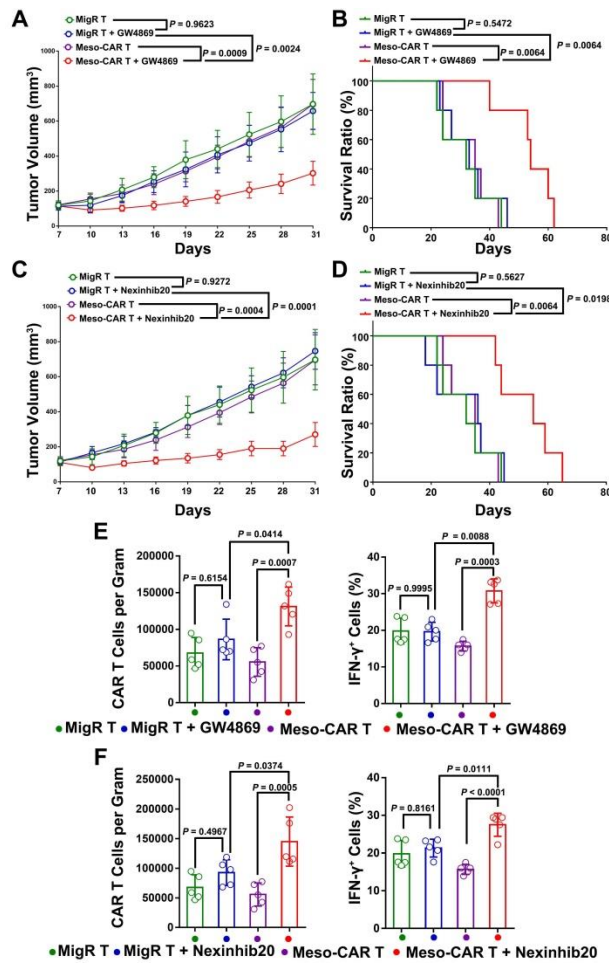
Figure S19. GW4869 and Nexinhib20 boosted CAR T therapy in NSG mouse model with PDAC. A, Related to GW4869 treatment, 4662 tumor growth in mice of indicated groups. **B,** Related to GW4869 treatment, survival rates of mice of indicated groups. **C,** Related to Nexinhib20 treatment, tumor growth in mice of indicated groups. **D,** Related to Nexinhib20 treatment, survival rates of mice of indicated groups. **E,** Related to GW4869 treatment, quantification of flow cytometry analysis of the number of Meso-CART cells in tumors for each group of mice (left panel), and the percentages of IFN-γ$^+$ Meso-CART cells (right panel). **F,** Related to Nexinhib20 treatment, quantification of flow cytometry analysis of the number of Meso-CART cells in tumors for each group of mice (left panel), and the percentages of IFN-γ$^+$ Meso-CART cells (right panel). Data represent mean ± s.d. (n=5). Statistical analysis is performed using Welch ANOVA with Dunnett's T3 multiple comparison tests **(A, C, E, F)** or log-rank test **(B, D)**.
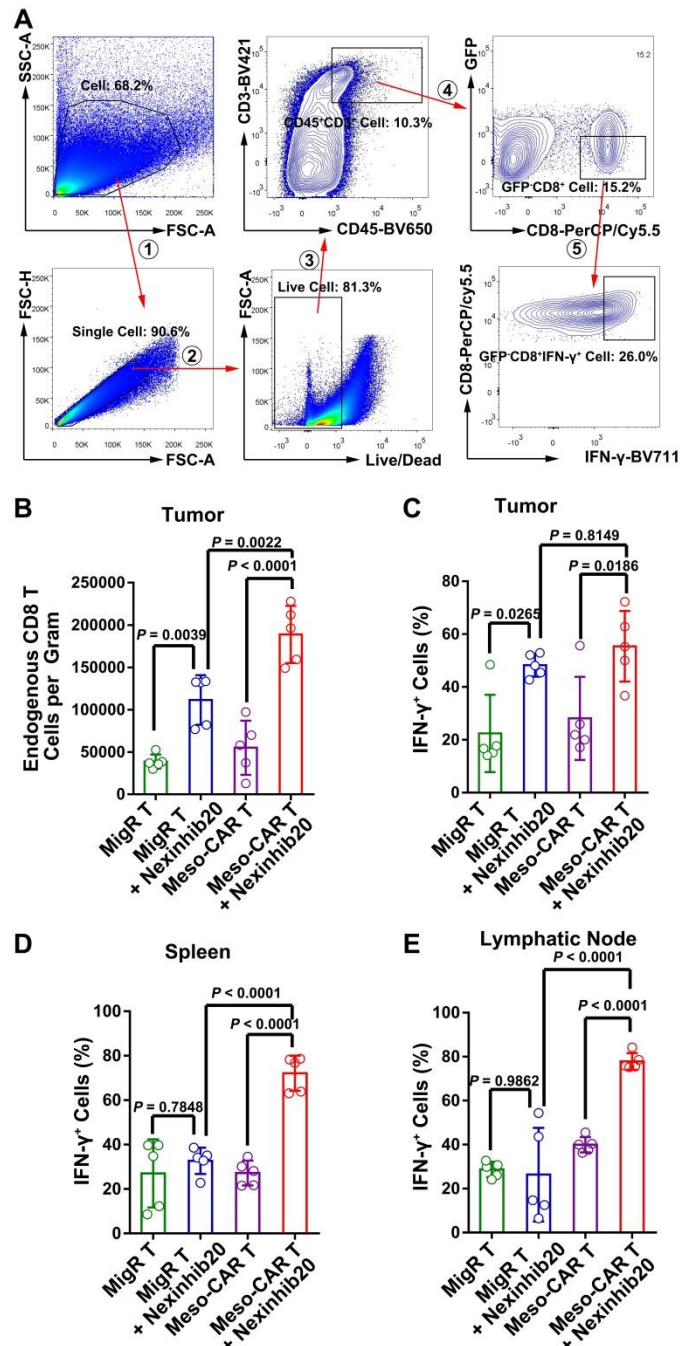
Figure S20. Combination of Meso-CAR T cells and Nexinhib20 systemically enhanced the activation of CD8 T cells in immune competent mice with PDAC. A, Representative contour plots showing the general gating strategy used in the analysis of total CD8 T cells and IFN-γ[+] CD8 T cells in C57BL/6 mice with 4662 xenografts. **B,** The number of CD8 T cells in tumors for each group of mice quantified from flow cytometry analysis. **C-E,** The percentage of IFN-γ[+] CD8 T cells in tumors (**C**), spleen (**D**) and lymphatic nodes (**E**) as quantified by flow cytometry. Data represent mean ± s.d. (n=5). Statistical analysis is performed using Welch ANOVA with Dunnett's T3 multiple comparison **(B-E)**.
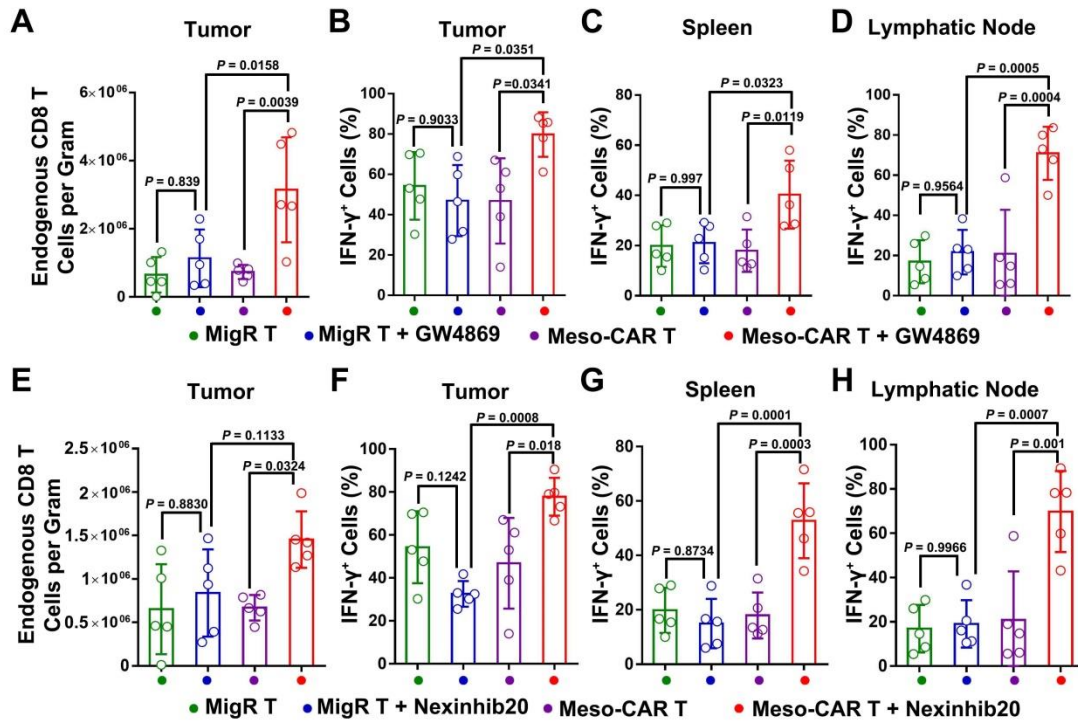
Figure S21. Combination of Meso-CAR T cells and GW4869 or Nexinhib20 systemically enhanced the activation of CD8 T cells in immune competent mice with MOC1 tumors. A, The number of CD8 T cells in tumors for each group of mice quantified from flow cytometry analysis. **B-D,** The percentage of IFN-γ+ CD8 T cells in tumors (**B**), spleen (**C**) and lymphatic nodes (**D**) as quantified from flow cytometry. **E,** The number of CD8 T cells in tumors for each group of mice quantified from flow cytometry analysis. **F-H,** The percentage of IFN-γ+ CD8 T cells in tumors (**F**), spleen (**G**) and lymphatic nodes (**H**) as quantified from flow cytometry. Data represent mean ± s.d. (n=5). Statistical analysis is performed using Welch ANOVA with Dunnett's T3 multiple comparison **(A-H).**

Table S1. Antibody Information

Antibody	Provider	Application	Dilution	Identifier
Anti-mouse mesothelin	Abcam	WB	1 : 10000	Cat#: ab213174 RRID:N/A
Anti-mouse mesothelin, biotin	Biorbyt	Depletion	1 : 20	Cat#: orb241037 RRID:N/A
Anti-mouse PD-L1	Cell Signaling Technology	WB, TEM	1 : 10000	Cat#: 60475 RRID:AB_2924680
Anti-mouse mesothelin	Thermo Fisher	Blocking, WB, TEM	10 µg/ml for Blocking; 1 : 10000 for WB; 1: 50 for TEM	Cat#: MA5-38575 RRID:AB_2898487
Anti-mouse CD63	Abcam	WB	1 : 10000	Cat#: ab217345 RRID:AB_2754982
Anti-mouse PD-L1	Bio X Cell	Blocking	10 µg/ml	Cat#: BE0101; RRID:AB_10949073
Mouse IgG isotype control	BioLegend	Blocking	10 µg/ml	Cat#: 401404 RRID:N/A
Rat IgG isotype control	Bio X Cell	Blocking	10 µg/ml	Cat#: BE0090 RRID:AB_1107780
Anti-mouse IFN-γ	BioLegend	FCM	1 : 50	Cat#:505836 RRID:AB_2650928
Anti-mouse TNF-α	BioLegend	FCM	1 : 50	Cat#: 506344 RRID:AB_2565953
Anti-active Caspase-3	BD Biosciences	FCM	1 : 50	Cat#: 560901; RRID:AB_10563896
Anti-human Ki-67	BD Biosciences	FCM	1 : 100	Cat#: 561283 RRID:AB_10716060
Anti-human Granzyme B	Thermo Fisher	FCM	1 : 100	Cat#: GRB04 RRID:AB_2536538
Anti-mouse Ki-67	BioLegend	FCM	1 : 50	Cat#: 652420 RRID:AB_2564285
Anti-mouse Granzyme B	eBioscience	FCM	1 : 50	Cat#: 12-8898-82 RRID:AB_10870787
Anti-human TNF-α	BioLegend	FCM	1 : 100	Cat#: 502944 RRID:AB_2562870
Anti-human IFN-γ	BioLegend	FCM	1 : 100	Cat#: 502538 RRID:AB_2563608

Anti-mouse CD8	BioLegend	FCM	1 : 100	Cat#: 126610 RRID:AB_2260149
Anti-mouse CD3	BioLegend	FCM	1 : 100	Cat#:100228 RRID:AB_2562553
Anti-mouse CD8	Cell Signaling Technology	IF	1 : 100	Cat#: 98941 RRID:AB_2756376
Anti-human CD63	Abcam	WB	1 : 1000	Cat#: ab134045 RRID:AB_2800495
Anti-Hrs	Cell Signaling Technology	WB	1 : 1000	Cat#: 15087S RRID:N/A
Anti-TSG101	Abcam	WB	1 : 1000	Cat#: ab125011 RRID:AB_10974262
Anti-human PD-L1	Cell Signaling Technology	WB	1 : 1000	Cat#: 13684S RRID:N/A
Anti-human CD9	Cell Signaling Technology	WB	1 : 1000	Cat#: 13174S RRID:N/A
Anti-GAPDH	Cell Signaling Technology	WB	1 : 2000	Cat#: 5174S RRID:N/A
Anti-Mouse IgG, F(ab')$_2$ fragment specific	Jackson ImmunoResearch	FCM	1 : 100	Cat#: 115-475-072 RRID:N/A
Anti-active Caspase-3	BD Biosciences	FCM	1 : 50	Cat#: 560626 RRID:AB_1727414
Anti-Trastuzumab	R&D Systems	FCM	1 : 100	Cat#: FAB95471R RRID:N/A
Anti-GFP	Cell Signaling Technology	WB	1 : 1000	Cat#: 2956 RRID:AB_1196615
Anti-CD19	Cell Signaling Technology	WB	1 : 1000	Cat#: 90176 RRID:AB_2800152
Anti-mouse CD25	BioLegend	FCM	1:100	Cat#: 102038 RRID: AB_2563060
Anti-mouse CD69	eBioscience	FCM	1:100	Cat#: 12-0691-82 RRID:AB_465732
Anti-mouse mesothelin	LSBio	FCM	1 : 100	Cat#: LS-C179484-100 RRID:N/A

WB: Western Blotting; IF: Immunofluorescence; FCM: Flow cytometry.